

Long-Range Kinetic Effects on the Alternating Ring Opening Metathesis of Bicyclo[4.2.0]oct-6-ene-7-carboxamides and Cyclohexene

Francis O. Boadi and Nicole S. Sampson*

Cite This: *ACS Org. Inorg. Au* 2023, 3, 233–240

Read Online

ACCESS |



Metrics & More



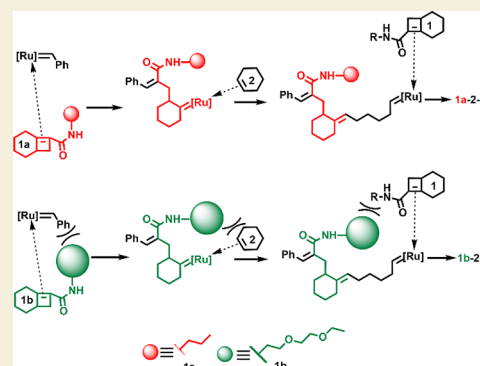
Article Recommendations



Supporting Information

ABSTRACT: We report an investigation of rates of ruthenium-catalyzed alternating ring opening metathesis (AROM) of cyclohexene with two different Ru-cyclohexylidene carbenes derived from bicyclo[4.2.0]oct-6-ene-7-carboxamides (A monomer) that bear different side chains. These monomers are propylbicyclo[4.2.0]oct-6-ene-7-carboxamide and *N*-(2-(2-ethoxyethoxy)ethanyl)bicyclo[4.2.0]oct-6-ene-7-carboxamide. The amide substitution of these monomers directly affects both the rate of the bicyclo[4.2.0]oct-6-ene-7-carboxamide ring opening and the rate of reaction of the resulting carbene with cyclohexene (B monomer). The resulting Ru-cyclohexylidenes underwent reversible ring opening metathesis with cyclohexene. However, the thermodynamic equilibrium disfavored cyclohexene ring opening. Utilization of triphenylphosphine forms a more stable PPh₃ ligated complex, which suppresses the reverse ring closing reaction and allowed direct measurements of the forward rate constants for formation of various A-B and A-B' complexes through carbene-catalyzed ring-opening metathesis and thus gradient polymer structure-determining steps. The relative rate of the propylbicyclo[4.2.0]oct-6-ene-7-carboxamide ring opening is 3-fold faster than that of the *N*-(2-(2-ethoxyethoxy)ethanyl)bicyclo[4.2.0]oct-6-ene-7-carboxamide. In addition, the rate of cyclohexene ring-opening catalyzed by the propyl bicyclooctene is 1.4 times faster than when catalyzed by the ethoxyethoxy bicyclooctene. Also, the subsequent rates of bicyclo[4.2.0]oct-6-ene-7-carboxamide ring opening by propyl-based Ru-hexylidene are 1.6-fold faster than ethoxyethoxy-based Ru-hexylidene. Incorporation of the rate constants into reactivity ratios of bicyclo[4.2.0]amide-cyclohexene provides prediction of copolymerization kinetics and gradient copolymer structures.

KEYWORDS: alternating ring opening metathesis, amide substitution, intermediate trapping, ruthenium cyclohexylidene, triphenylphosphine, NMR spectroscopy



Ring opening metathesis polymerization (ROMP) of cyclic olefins is a thermodynamically controlled chemical transformation. The unfavorable entropy associated with polymerization disfavors ring-opening polymerization of cyclic olefins with low ring strain energies.¹ Hence, ROMP has been limited to high strain energy monomers such as norbornenes, cyclooctadienes, and cyclobutenes.^{1–3} However with recent developments and innovations, low strain cyclic olefins such as cyclohexene (CH), which traditionally is impractical for ROMP,⁴ can be incorporated into alternating copolymers via ROMP (AROMP)^{5–7} and cascade enyne metathesis polymerization.^{8–10} When CH is combined with specific monomer types that undergo only a single metathesis cycle and do not homopolymerize, the monomers will cross-react to form precisely alternating copolymers.^{5–7} Bicyclooctenes^{6,11} and disubstituted cyclopropenes⁷ are prominent examples of single addition monomers that can form highly alternating copolymers with cyclohexene and other low strain cyclic olefins. This innovation provides rapid access to copolymers with well-

defined backbone sequences^{12,13} and copolymers with backbone degradability.^{14,15}

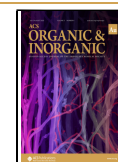
AROMP has been used to create materials with unique and interesting properties.^{12,13,16} However, in order to create more advanced functional materials using AROMP, it is important that we understand the kinetics of the ring openings of the bicyclooctene and the subsequent ring opening of CH. For a Ru-catalyst to effectively ring open CH, the equilibrium should be shifted toward the metathesis product.⁴ α -Carbonyl containing ruthenium carbene complexes^{4,6,17–19} meet this criteria because of their ability to stabilize their complexes through the carbonyl group.

Received: March 26, 2023

Revised: May 16, 2023

Accepted: May 17, 2023

Published: May 30, 2023



The third-generation Ru-alkylidene catalyst reacts with bicyclo-oct-7-ene-7-carboxylate to generate an enoic carbene,⁶ which efficiently ring opens CH and yields a linear-alternating copolymer. However, when bicyclo[4.2.0]oct-6-ene-7-carboxamide reacts with the ruthenium benzylidene complex (Chart 1), it generates Ru-cyclohexylidene carbene (Figure 1).^{13,20}

Chart 1. Kinetic Studies Performed with Bicyclo[4.2.0]-oct-6-ene-7-carboxamides with a Propyl Amide Substituent (1a) and *N*-(2-(2-Ethoxyethoxy)ethanyl Amide Substituent (1b), the Low-Strain Cyclohexene (2), and I as the Metathesis Catalyst

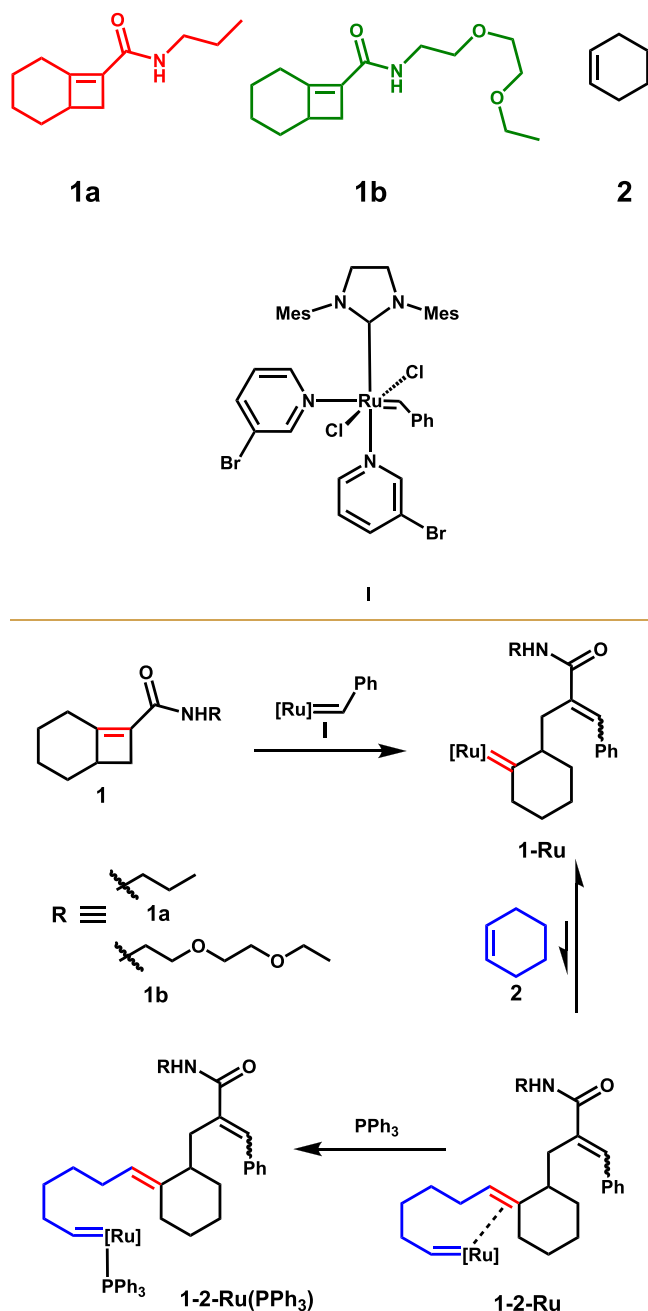


Figure 1. AROM of bicyclo[4.2.0]oct-6-ene-7-carboxamide. PPh_3 was used to kinetically trap the ring opened product **1-alt-2-Ru** to shift the equilibrium to ring opened species in the absence of additional **1** monomer.

Although not an α -carbonyl containing carbene, the Ru-cyclohexylidene can react with cyclohexene²⁰ in the presence of additional bicyclo[4.2.0]oct-6-ene-7-carboxamide monomers to form a linear-alternating copolymer.^{11–13} To this end, we employed bicyclo[4.2.0]oct-6-ene-7-carboxamide systems in extensive studies because of their fast ROM reactivities compared with previous bicyclo[4.2.0] systems.⁶

The ring opening rates of bicyclo[4.2.0]oct-6-ene-7-carboxamides are directly influenced by amide substitution.^{12,13} In the mixed copolymerization of **1a**, **1b**, and **2**, the rate of formation of **1a-2-1a** was 6-fold faster than **1b-2-1b**, resulting in the formation of a gradient copolymer.¹³ However, the rate of ROM for propylbicyclo[4.2.0]oct-6-ene-7-carboxamide (**1a**) is only 3-fold faster than for *N*-(2-(2-ethoxyethoxy)ethanyl bicyclo[4.2.0]oct-6-ene-7-carboxamide (**1b**).¹³ Thus, there are longer-range effects beyond the reactivity of the **1** monomer. In this work, we investigate the kinetics of ring opening of cyclohexene by the two different Ru-cyclohexylidene complexes (**1-Ru**) and the subsequent ring opening of bicyclo[4.2.0]oct-6-ene-7-carboxamides by (**1-2-Ru**) to elucidate the rates of individual steps and to understand the extent of long-range influence on the metathesis rate as a first step in designing selectivity for gradient copolymerization in the AROM system.

RESULTS AND DISCUSSION

To understand the kinetics of AROM of bicyclo[4.2.0]oct-6-ene-7-carboxamides, we undertook analysis of the first ROM of bicyclo[4.2.0]oct-6-ene-7-carboxamide, the subsequent ROM of cyclohexene, and the second ROM of bicyclo[4.2.0]oct-6-ene-7-carboxamide. We prepared two bicyclo[4.2.0]oct-6-ene-7-carboxamides: one with a propyl side chain (**1a**) and the other with a *N*-(2-(2-ethoxyethoxy)ethanyl side chain (**1b**) via acid–amine coupling.¹³ The ruthenium third-generation catalyst (**I**) was used as the metathesis catalyst.

Kinetics of Ring Opening (ROM) of 1

We first analyzed the kinetics of the initial ROM of **1** by **I** under pseudo-first-order conditions. The initiator **I** was allowed to react with excess **1**.²¹ The reactions were conducted at 40 °C in CDCl_3 and monitored by ^1H NMR spectroscopy by following the disappearance of the Ru-benzylidene proton signal at 19.1 ppm. This signal was integrated against protons in the NHC ligand (Figure S1). The reactions of **1** with **I** to yield the Ru-cyclohexylidene complex (**1-Ru**) were second-order overall with first-order dependence on both the concentration of **I** and of **1** ($d[\mathbf{1-Ru}]/dt = k[\mathbf{I}][\mathbf{1}]$; Figure 2 and Figure S2). The ROM second-order rate constant for **1a** is $12.9 \text{ M}^{-1} \text{ min}^{-1}$, which is about 3-fold faster than for **1b** ($k = 3.95 \text{ M}^{-1} \text{ min}^{-1}$). The slower ROM reactivity of **1b** can be attributed to the greater steric bulk of its side chain. These results are consistent with previous measurements made under second-order conditions.¹³

Kinetics of Ring Opening of Cyclohexene (2) (AROM)

To determine the kinetics of the ring opening of cyclohexene **2**, first **1** and **I** were allowed to react at equimolar concentrations to stoichiometrically generate **1-Ru**. The generation of **1-Ru** was confirmed by disappearance of the Ru-benzylidene proton signal at 19.1 ppm (^1H NMR) and the appearance of the Ru-cyclohexylidene carbon signal at 158.3 ppm (^{13}C NMR, Figure 3). When >90% of **1-Ru** had formed, it was then allowed to react with excess **2** (about 10 equiv). The reactions were followed using ^1H and ^{13}C NMR spectroscopy

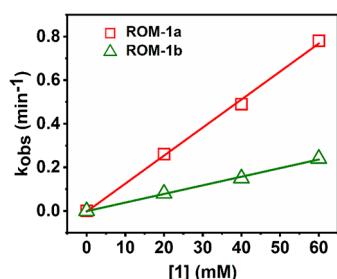


Figure 2. Plots of k_{obs} for ROM of **1** as a function of concentration of **1**. The slopes of the best-fit lines ($k_{\text{obs}} = k[\mathbf{1}]$, $R^2 = 0.99$) represent second-order rate constants of 12.9 ± 0.4 and $3.95 \pm 0.1 \text{ M}^{-1} \text{ min}^{-1}$ for ROM of **1a** (square, red line) and ROM of **1b** (triangle, green line), respectively. Reactions were conducted at 40°C in CDCl_3 .

(Figure 3). The formation of **1-alt-2-Ru** (or **1-2-Ru**) was confirmed by the appearance of a new multiplet alkylidene proton signal Hb at 19.0 ppm (^1H NMR, Figure 3). However, no more than 20% conversion was observed even after 4 h. The formation of **1-2-Ru** could not be detected by ^{13}C NMR spectroscopy (no peak observed near 332 ppm), presumably due to its low concentration. This observation is in agreement with the assertion that ring opening of cyclohexene by Ru-alkylidene is thermodynamically unfavorable and that the equilibrium favors the cyclohexene.¹⁸ It is important to note that upon addition of cyclohexene, the benzylidene proton

signal (Ha) shifted slightly downfield, suggesting that the cyclohexene may coordinate with **1-Ru** without undergoing ring opening since the concentration of **1** did not change (Figure 3, Figures S3 and S4). Hence, the small concentrations of **1** present in the reaction mixtures do not interfere with the subsequent reactions.

In order to accurately measure the forward rate of the metathesis reaction: ring opening of cyclohexene by cyclohexylidene **1-Ru**, triphenylphosphine PPh_3 , a strong σ -donating,²² labile ligand²³ that is inexpensive and easy to handle, was added to the reaction mixture. We anticipated that PPh_3 will bind to the Ru center^{1,24} of **1-2-Ru** and form a more stable PPh_3 ligated complex (**1-2-Ru(PPh₃)**), thus suppressing the reverse ring closing reaction (Figure 1). When 10 equiv of PPh_3 was added to the reaction mixture, the rate of formation of **1-2-Ru(PPh₃)** increased significantly, consistent with suppression of the reverse reaction. Specifically, the observed rate of ring opening was increased by 4-fold and 3-fold for **1a-2-Ru(PPh₃)** and **1b-2-Ru(PPh₃)**, respectively (Figure 3). ^{31}P NMR spectra showed that PPh_3 is ligated to the ruthenium center (Figure S5).

We determined the rate constants for ring opening of **2** by **1-Ru** under pseudo-first-order conditions. First, **1-Ru** was generated by reacting equimolar amounts of **1** and **1**. A molar excess of PPh_3 was added to the reaction mixture followed by addition of **2** at varying concentrations. Small aliquots were removed at specified time intervals and quenched

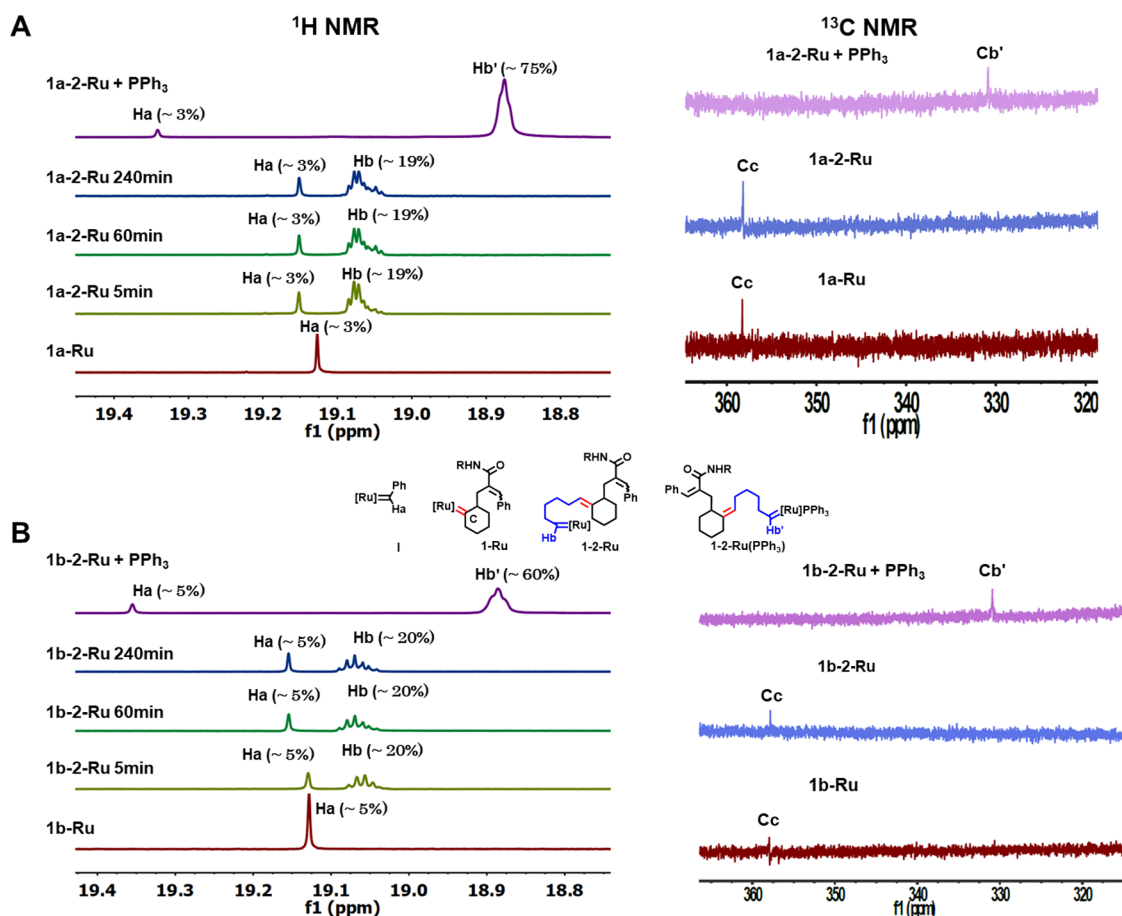


Figure 3. ^1H (left) and ^{13}C (right) NMR spectra of the ring opening of **2** with **1-Ru**. ROM of **2** is not favored but with addition of PPh_3 , the equilibrium for ring opening of **2** shifts 4-fold for **1a-2** (A) and 3-fold for **1b-2** (B). Reactions were conducted at 40°C in CDCl_3 .

immediately with ethyl vinyl ether. After removing solvents, the quenched crude mixture was analyzed using ^1H NMR spectroscopy. Ring opening of cyclohexene was judged by the disappearance of [1-Ru], which was analyzed by integrating the resonances for cyclohexylmethylene protons (Ha & Hb) at 4.65–4.55 ppm against those for the side chain methylene protons, Hc (2H in the case of **1a**), and Hc-g (10H in the case of **1b**) (Figures S6 and S7). The progress of the reaction was monitored by the disappearance of cyclohexylmethylene protons (Ha & Hb) (Figures S8 and S9). To ensure that the rate measured is for ring opening of cyclohexene and not the reaction of PPh_3 , we doubled the equivalents of PPh_3 used (Figures S10 and S11). The rate of ring opening of cyclohexene did not change even as PPh_3 concentration was doubled. This confirms that PPh_3 addition does not influence the AROM and that the rate constants measured are truly the forward rate constants of the ring opening of cyclohexene.

The rate of ring opening of **2** increased by the same factor by which the concentration of **2** was increased (Figure S12), which indicates that ring opening of **2** with 1-Ru has a first-order dependence on the concentration of **2**. A plot of the observed rate constant (k_{obs}) as a function of concentration of **2** was linear, which indicates the overall reaction kinetics are second-order. The rates of formation of 1-2 (defined as $d[1\text{-}2\text{-Ru}(\text{PPh}_3)]/dt = k[1\text{-Ru}][2]$) have rate constants of $0.38 \text{ M}^{-1} \text{ min}^{-1}$ for 1a-2-Ru(PPh_3) and $0.27 \text{ M}^{-1} \text{ min}^{-1}$ for 1b-2-Ru(PPh_3) (Figure 4). The ring opening of **2** with 1a-Ru is 1.4

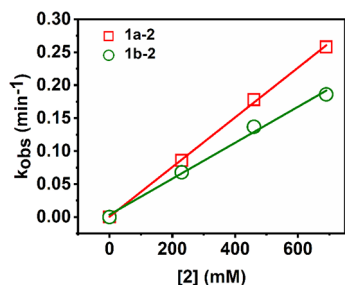


Figure 4. AROM of cyclohexene is first-order in cyclohexene. Plots of k_{obs} of ring opening metathesis of **2** as a function of concentration of **2** at a fixed concentration of 1-Ru (23 mM). The slopes of the best-fit lines ($k_{\text{obs}} = k[2]$, $R^2 = 0.99$) provide second-order rate constants of 0.38 ± 0.01 and $0.27 \pm 0.01 \text{ M}^{-1} \text{ min}^{-1}$ for ROM of **2** by 1a-Ru (red line) and 1b-Ru (green line), respectively.

times faster than with 1b-Ru. The rate of ring opening of cyclohexene is much slower than the rate of ring opening of bicyclo[4.2.0]oct-6-ene-7-carboxamide (Figure 5).

Thus, in the AROM formation pathway, ring opening of **2** is the rate-determining step. We noted that without kinetically trapping the ring opened product, the formation of 1-2-Ru was disfavored. In the case of a polymerization (AROMP) reaction, the driving force necessary is provided by having an excess of **1** and **2** relative to **I**. We propose the origin of AROM or AROMP in Figure 6.

The formation of the 1-1 dimer through pathway I is kinetically disfavored due to steric repulsion^{25,26} and possibly substrate distortion. Kinetically, pathway II leading to the formation of 1-2-Ru is favorable. However, formation of product 1-2-Ru is thermodynamically disfavored. Nonetheless, the presence of excess monomers (the norm in a polymerization reaction) provides a driving force for the forward

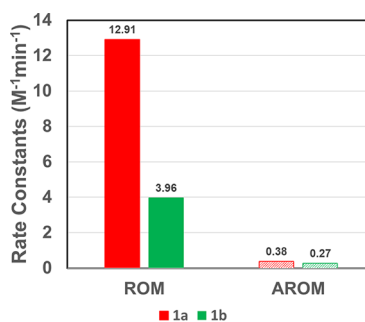
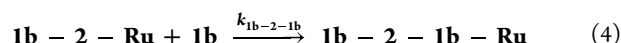
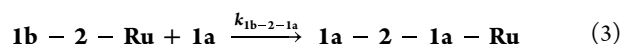
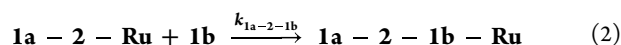
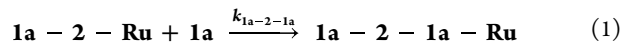


Figure 5. Comparison of rate constants for ROM and AROM. Rate constants for ROM: reaction of **1** with **I**; AROM: reaction of cyclohexene **2** with 1-Ru. The rate of ROM of **1a** is 3-fold faster than the rate of ROM of **1b**. The rate of AROM of **2** with **1a** is 1.4-fold faster than with **1b**.

reaction through complexation to the active ruthenium carbene species.

Copolymer Long-Range Effects on Monomer Incorporation

Copolymer composition and comonomer sequence distribution are important factors that dictate copolymer properties and functions.^{27–29} The distribution of comonomers in a copolymer is largely determined by the reactivity ratios of the comonomers, the tendency of an active chain end to add onto an identical monomer.³⁰ Assuming that the addition of bicyclo[4.2.0]oct-6-ene-7-carboxamides **1a** and **1b** is dependent on the identity of the terminal unit 1-2-Ru, four possible chain propagating equations must be considered (eqs 1–4).



Assuming a steady-state concentration of 1a-2-Ru and 1b-2-Ru, the reactivity ratios r_1 and r_2 can be defined as

$$r_1 = k_{1\text{a}-2-1\text{a}}/k_{1\text{a}-2-1\text{b}} \quad (5)$$

$$r_2 = k_{1\text{b}-2-1\text{b}}/k_{1\text{b}-2-1\text{a}} \quad (6)$$

To determine the rate constants $k_{1\text{a}-2-1\text{a}}$, $k_{1\text{a}-2-1\text{b}}$, $k_{1\text{b}-2-1\text{a}}$, and $k_{1\text{b}-2-1\text{b}}$, we performed a second ROM experiment. We monitored the kinetics of the second ring opening of bicyclo[4.2.0]oct-6-ene-7-carboxamide (**1''**) with 1-2-Ru to form 1-2-1''-Ru. First, we mixed bicyclo[4.2.0]amide **1** and initiator **I** in an equimolar ratio to form 1-Ru. Triphenylphosphine (30 equiv) and cyclohexene (**2**) (30 equiv) were added to generate 1-2-Ru(PPh_3). Using ^1H NMR spectroscopy, the formation of 1-2-Ru(PPh_3) was confirmed by the appearance of a new multiplet resonance at 18.9 ppm, which corresponds to the alkylidene proton. After 1-2-Ru(PPh_3) was formed, one equivalent of **1''** was added. The rate of formation of 1-2-1'' was monitored by the disappearance of a resonance at 2.95 ppm in the ^1H -NMR spectrum, which corresponds to the Ha proton of amide **1** (Figures S13 and S14). The kinetic data only fit the first-order integrated equation.

Since excess amounts of cyclohexene (**2**) were used, the cyclohexylidene species 1-2-1-Ru formed readily and reacts

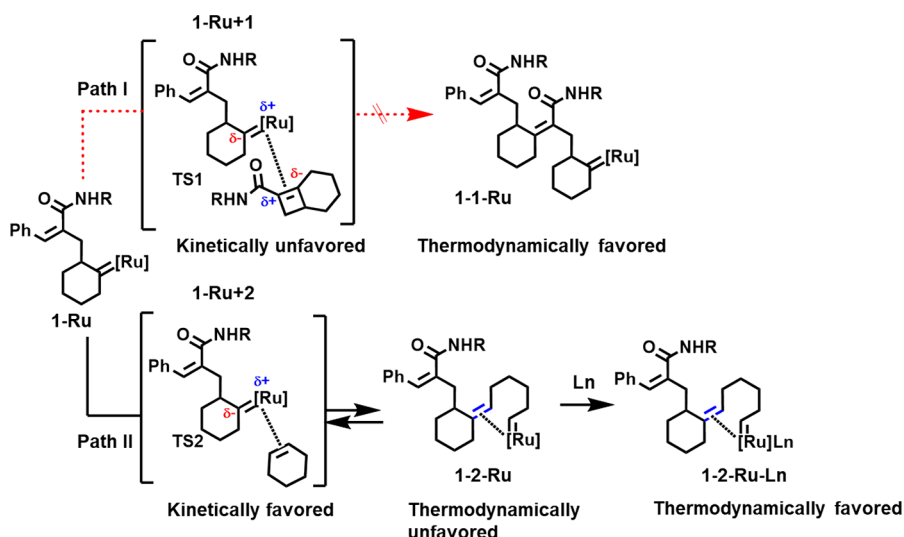


Figure 6. Proposed pathways for AROM reaction. Ln is the coupling agent, which is PPh_3 in the case of AROM study and **1** in the case of AROMP polymerization.

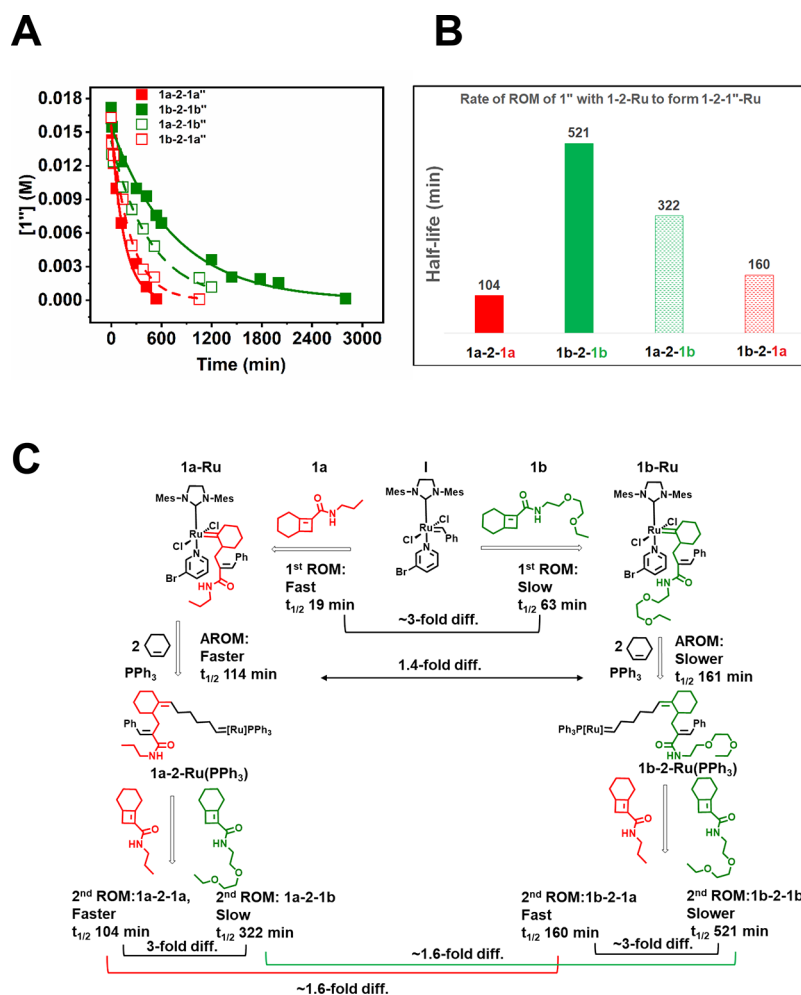


Figure 7. Summary of rates and species formed in the AROM copolymerization pathway. (A) Kinetics of the second ROM of **1''**: ROM of **1a** with **1a-2-Ru** to form **1a-2-1a''-Ru** (red solid line, $k_{\text{obs}} = 6.65 \times 10^{-3} \text{ min}^{-1}$), ROM of **1b** with **1a-2-Ru** to form **1a-2-1b''-Ru** (green dashed line, $k_{\text{obs}} = 2.15 \times 10^{-3} \text{ min}^{-1}$), ROM of **1b** with **1b-2-Ru** to form **1b-2-1b-Ru** (green solid line, $k_{\text{obs}} = 1.33 \times 10^{-3} \text{ min}^{-1}$), and ROM of **1a** with **1b-2-Ru** to form **1b-2-1a-Ru** (green dashed line, $k_{\text{obs}} = 4.32 \times 10^{-3} \text{ min}^{-1}$). (B) Comparison of the rates of second ROM of **1** with **1-2-Ru** to form **1-2-1''-Ru**. Colored letter denotes the appended [4.2.0] amide. (C) Schematic representation of the reactivities of different **1-Ru** complexes.

with **2** to regenerate the hexylidene, and therefore the concentration of **1-2-Ru** did not seem to change (as per the ^1H NMR proton signal at 18.9 ppm) even though **1** was consumed quantitatively (Figures S13–S16). Based on the kinetic plots (Figure 7), the rate constants of the second ROM are the following: $k_{1a-2-1a} = 6.65 \times 10^{-3} \text{ min}^{-1}$, $k_{1a-2-1b} = 2.15 \times 10^{-3} \text{ min}^{-1}$, $k_{1b-2-1b} = 1.33 \times 10^{-3} \text{ min}^{-1}$, and $k_{1b-2-1a} = 4.32 \times 10^{-3} \text{ min}^{-1}$. From eqs 5 and 6, the reactivity ratios can be computed: $r_1 = 3.09$ and $r_2 = 0.308$ (thus, $r_1 > 1 > r_2$). This is indicative of when these two bicyclo[4.2.0]oct-6-ene-7-carboxamides **1a** and **1b** are reacted with cyclohexene **2** under the catalysis of ruthenium alkylidene, gradient copolymers whose composition changes smoothly from **1a-2-1a** to **1b-2-1b** would be formed.^{31,32} The propensity of **1a-2-Ru** reacting with identical bicyclo[4.2.0]amide **1a** is much more likely than **1b-2-Ru** reacting with **1b** (a 5-fold difference). Inherently, there is a 3-fold difference between the ring opening of **1a** and **1b**; however, geometric constraints of the reactive species **1-2-Ru** contribute an additional 1.6-fold difference (**1a-2-Ru** vs **1b-2-Ru**) (Figure 7C). In addition, the rate of ROM of **1a** by **1b-2-Ru** is 2-fold faster than the rate of ROM of **1b** by **1a-2-Ru**, which indicates that cross propagation would favor **1b-2-1a** formation over **1a-2-1b**. This is interesting because if **1b-2-Ru** were to form, it would readily react with **1a**. These kinetic data imply that a terpolymerization reaction of **1a**, **1b**, and **2** catalyzed by **I** would yield predominantly **1a-2** microsequences with intermittent microsequences of **1b-2** in the initial stage and when **1a** is almost completely consumed, then longer microsequences of **1b-2** would be formed. This phenomenon is consistent with gradient copolymerization.¹³ The inherent 3-fold difference in ROM of **1a** vs **1b**, 1.4-fold difference in ring opening of **2** by **1a-Ru** vs **1b-Ru**, and the 1.6-fold difference due to the steric constraints of the terminal active species may contribute to the 6-fold difference in the formation of **1a-2-1a** vs **1b-2-1b** microsequences in copolymerization.¹³

CONCLUSIONS

Monomers with different reactivities are incorporated into copolymers at different rates, resulting in asymmetrical distribution of the comonomers in polymer chains. Steric hindrance is an important parameter that can differentiate the reactivities of two monomers. Other factors such as electronics may also contribute to the differences in reactivities among monomers. For bicyclo[4.2.0]oct-6-ene-7-carboxamides with similar strain energies, the most important contributing factor of reactivity is the substituent on the amide. In this work, we demonstrated that amide substitution has direct effects on all three ROM processes: ROM1 of bicyclo[4.2.0]carboxamide, ROM of cyclohexene, and ROM2 of bicyclo[4.2.0]carboxamide. The differences resulted in a cumulative 6-fold faster rate of formation of **1a-2-1b** vs **1b-2-1b**, which fits well with a gradient copolymerization model.¹³ The evidence presented here suggests that kinetic data from the three steps involved in the formation of **1-2-1** can be used as a predictive tool for gradient copolymerization. To accurately use this model to predict other copolymerization types, we are currently investigating other [4.2.0] amides with different side chains. We will test them for their ROM1 and ROM2 reactivities and the reactivities of ring opening of cyclohexene. The cumulative rates of formation of A-B-A' complexes as well as the reactivity ratios of A-B complexes can be computed from the kinetic reactions outlined here and can be used to predict

the copolymer type formed when two different A monomers and a B monomer are polymerized using ruthenium alkylidene as the catalyst.

EXPERIMENTAL SECTION

Materials and General Methods

Metathesis reactions were performed under a N_2 atmosphere. Grubbs 2nd generation catalyst ($\text{Cl}_2(\text{H}_2\text{IMes})(\text{PCy}_3)\text{Ru} = \text{CHPh}$) and deuterated trichloromethane (CDCl_3) were purchased from Aldrich. Grubbs 3rd generation catalyst ($3\text{-BrPyr})_2\text{Cl}_2(\text{H}_2\text{IMes})\text{Ru} = \text{CHPh}$ (**I**) was prepared from 2nd generation catalyst and 3-bromopyridine.³³ Propyl[4.2.0]oct-6-ene-7-carboxamide (**1a**)¹⁴ and *N*-(2-(2-ethoxyethoxy)ethanyl)bicyclo[4.2.0]oct-6-ene-7-carboxamide (**1b**)¹³ were prepared according to the literature, and both ^1H and ^{13}C NMR data were in agreement with the literature. Dry, oxygen-free CH_2Cl_2 was prepared with a Pure Process Technology solvent purification system. Mallinckrodt silica gel-60 (230–400 mesh) was used for column chromatography. Analytical thin-layer chromatography was performed on precoated silica gel plates (60F254) and Combi-Flash chromatography on RediSep normal-phase silica columns (silica gel-60, 230–400 mesh). NMR spectra were recorded at ^1H -500 MHz and ^{13}C -125 MHz and ^1H -700 MHz and ^{13}C -176 MHz. Chemical shifts were recorded relative to the CDCl_3 peak.

General Procedure for Monitoring 1st ROM Kinetics

Reactions were run in NMR tubes in deuterated trichloromethane and tubes capped with a septum. All reagents were added by a syringe. Reaction mixtures were maintained at 40 °C (using a water bath) under a N_2 atmosphere, and at the indicated time intervals, ^1H -NMR spectra were collected. Spectra were integrated, the reaction progress was plotted as concentration of [**I**] vs time (min), and the data were fit to a first-order integrated rate law equation.

1st ROM Kinetics for 1a. 1:1a (1:5). A spectrum for reaction time $t = 0$ min of a solution of **I** (2.5 mg, 2.8 μmol) in deuterated trichloromethane (500 μL) was recorded by ^1H -NMR spectroscopy at 40 °C. A solution of **1a** in deuterated trichloromethane (2.7 mg, 14.0 μmol , 200 μL) was added rapidly into the NMR tube, the contents were mixed, and the reaction was monitored.

1:1a (1:10). A spectrum for reaction time $t = 0$ min of a solution of **I** (2.5 mg, 2.8 μmol) in deuterated trichloromethane (500 μL) was recorded by ^1H -NMR spectroscopy at 40 °C. A solution of **1a** in trichloromethane (5.5 mg, 28.5 μmol , 200 μL) was added rapidly into the NMR tube, the contents were mixed, and the reaction was monitored.

1:1a (1:15). A spectrum for reaction time $t = 0$ min of a solution of **I** (2.5 mg, 2.8 μmol) in deuterated trichloromethane (500 μL) was recorded by ^1H -NMR spectroscopy at 40 °C. A solution of **1a** in trichloromethane (8.2 mg, 42.4 μmol , 200 μL) was added rapidly into the NMR tube, the contents were mixed, and the reaction was monitored.

1st ROM Kinetics for 1b. 1:1b (1:5). A spectrum for reaction time $t = 0$ min of a solution of **I** (2.5 mg, 2.8 μmol) in deuterated trichloromethane (500 μL) was recorded by ^1H -NMR spectroscopy at 40 °C. A solution of **1b** in trichloromethane (3.8 mg, 14.2 μmol , 200 μL) was added rapidly into the NMR tube, the contents were mixed, and the reaction was monitored.

1:1b (1:10). A spectrum for reaction time $t = 0$ min of a solution of **I** (2.5 mg, 2.8 μmol) in deuterated trichloromethane (500 μL) was recorded by ^1H -NMR spectroscopy at 40 °C. A solution of **1b** in trichloromethane (7.6 mg, 28.4 μmol , 200 μL) was added rapidly into the NMR tube, the contents were mixed, and the reaction was monitored.

1:1b (1:15). A spectrum for reaction time $t = 0$ min of a solution of **I** (2.5 mg, 2.8 μmol) in deuterated trichloromethane (500 μL) was recorded by ^1H -NMR spectroscopy at 40 °C. A solution of **1b** in trichloromethane (11.4 mg, 42.6 μmol , 200 μL) was added rapidly into the NMR tube, the contents were mixed, and the reaction was monitored.

General Procedure for Monitoring AROM Kinetics

Reactions were run in 2 mL glass vials in trichloromethane and vials capped with a septum. All reagents were added by a syringe. Reaction mixtures were maintained at 40 °C (using a water bath) under a N₂ atmosphere. Aliquots (50 μ L) were removed at indicated time intervals and quenched immediately with excess ethyl vinyl ether. Solvents were removed in vacuo, and the crude reaction mixture was redissolved in deuterated trichloromethane (CDCl₃) and analyzed by ¹H NMR spectroscopy. The concentration of **1-Ru** remaining was plotted as a function of time, and data were fit with a first-order integrated rate law equation.

Alternating ROM (AROM) Kinetics for Cyclohexene

1a-2 or 1b-2:Cyclohexene (1:10). A solution of **I** (15 mg, 17 μ mol) in dichloromethane (500 μ L) was added to a vial containing 170 μ L of **1a** (3.3 mg, 17 μ mol) or **1b** (4.6 mg, 17 μ mol) and allowed to react at 40 °C for approx. 8 h when the Ru-benzylidene proton signal in the ¹H NMR spectrum integrated $\leq 5\%$ of its starting concentration. An aliquot (70 μ L) was removed and immediately quenched with excess ethyl vinyl ether. To the remaining mixture (containing approx. 15 μ mol **1a-Ru** or **1b-Ru**), a solution (50 μ L) of triphenylphosphine (39 mg, 150 μ mol) and cyclohexene **2** (15 μ L, 150 μ mol) was added, the contents were mixed, and the reaction was monitored.

1a-2 or 1b-2:Cyclohexene (1:20). A solution of **I** (15 mg, 17 μ mol) in dichloromethane (500 μ L) was added to a vial containing 170 μ L of **1a** (3.3 mg, 17 μ mol) or **1b** (4.6 mg, 17 μ mol) and allowed to react at 40 °C for approx. 8 h when the Ru-benzylidene proton signal in the ¹H NMR spectrum integrated $\leq 5\%$ of its starting concentration. An aliquot (70 μ L) was removed and immediately quenched with excess ethyl vinyl ether. To the remaining mixture (containing approx. 15 μ mol **1a-Ru** or **1b-Ru**), a solution (50 μ L) of triphenylphosphine (78 mg, 300 μ mol) and cyclohexene **2** (30 μ L, 300 μ mol) was added, the contents were mixed, and the reaction was monitored.

1a-2 or 1b-2:Cyclohexene (1:30). A solution of **I** (15 mg, 17 μ mol) in dichloromethane (500 μ L) was added to a vial containing 170 μ L of **1a** (3.3 mg, 17 μ mol) or **1b** (4.6 mg, 17 μ mol) and allowed to react at 40 °C for approx. 8 h when the Ru-benzylidene proton signal in the ¹H NMR spectrum integrated $\leq 5\%$ of its starting concentration. An aliquot (70 μ L) was removed and immediately quenched with excess ethyl vinyl ether. To the remaining mixture (containing approx. 15 μ mol **1a-Ru** or **1b-Ru**), a solution (50 μ L) of triphenylphosphine (118 mg, 450 μ mol) and cyclohexene **2** (45 μ L, 450 μ mol) was added, the contents were mixed, and the reaction was monitored.

General Procedure for Monitoring 2nd ROM Kinetics

Reactions were run in NMR tubes in deuterated trichloromethane and tubes capped with a septum. All reagents were added by a syringe. Reaction mixtures were maintained at 40 °C under a N₂ atmosphere, and at the indicated time intervals, ¹H-NMR spectra were collected. Spectra were integrated, the reaction progress was plotted as concentration of [**1''**] vs time (min), and the data were fit with a first-order integrated rate law equation. **1''** is the second equivalent of monomer **1** after formation of a **1-2-Ru(PPh₃)** complex.

2nd ROM Kinetics for 1'' with 1-2-Ru(PPh₃) to Form 1-2-1''-Ru(PPh₃). **1a-2-1a-Ru(PPh₃).** A solution of **I** (15 mg, 17 μ mol) in deuterated trichloromethane (500 μ L) was added to an NMR tube containing a solution (200 μ L) of **1a** (3.3 mg, 17 μ mol) and allowed to react at 40 °C for approx. 8 h when the Ru-benzylidene proton signal in the ¹H NMR spectrum integrated $\leq 5\%$ of its starting concentration. A solution (150 μ L) of triphenylphosphine (118 mg, 450 μ mol) and cyclohexene **2** (45 μ L, 450 μ mol) was added, and the reaction was maintained at 40 °C. When **1a-2-Ru** was formed as judged by the appearance of a new multiplet proton signal at 19.05 ppm, a solution (200 μ L) of **1a''** (3.3 mg, 17 μ mol) was added, the contents were mixed, and the reaction was monitored.

1b-2-1b-Ru(PPh₃). A solution of **I** (15 mg, 17 μ mol) in deuterated trichloromethane (500 μ L) was added to an NMR tube containing a

solution (200 μ L) of **1b** (4.6 mg, 17 μ mol) and allowed to react at 40 °C for approx. 8 h when the Ru-benzylidene proton signal in the ¹H NMR spectrum integrated $\leq 5\%$ of its starting concentration. A solution (150 μ L) of triphenylphosphine (118 mg, 450 μ mol) and cyclohexene **2** (45 μ L, 450 μ mol) was added, and the reaction was maintained at 40 °C. When **1b-2-Ru** was formed as judged by the appearance of a new multiplet proton signal at 19.05 ppm, a solution (200 μ L) of **1b''** (4.6 mg, 17 μ mol) was added, the contents were mixed, and the reaction was monitored.

1a-2-1b-Ru(PPh₃). A solution of **I** (15 mg, 17 μ mol) in deuterated trichloromethane (500 μ L) was added to an NMR tube containing a solution (200 μ L) of **1a** (3.3 mg, 17 μ mol) and allowed to react at 40 °C for approx. 8 h when the Ru-benzylidene proton signal in the ¹H NMR spectrum integrated $\leq 5\%$ of its starting concentration. A solution (150 μ L) of triphenylphosphine (118 mg, 450 μ mol) and cyclohexene **2** (45 μ L, 450 μ mol) was added, and the reaction was maintained at 40 °C. When **1a-2-Ru** was formed as judged by the appearance of a new multiplet proton signal at 19.05 ppm, a solution (200 μ L) of **1b''** (4.6 mg, 17 μ mol) was added, the contents were mixed, and the reaction was monitored.

1b-2-1a-Ru(PPh₃). A solution of **I** (15 mg, 17 μ mol) in deuterated trichloromethane (500 μ L) was added to an NMR tube containing a solution (200 μ L) of **1b** (4.6 mg, 17 μ mol) and allowed to react at 40 °C for approx. 8 h when the Ru-benzylidene proton signal in the ¹H NMR spectrum integrated $\leq 5\%$ of its starting concentration. A solution (150 μ L) of triphenylphosphine (118 mg, 450 μ mol) and cyclohexene **2** (45 μ L, 450 μ mol) was added, and the reaction was maintained at 40 °C. When **1b-2-Ru** was formed as judged by the appearance of a new multiplet proton signal at 19.05 ppm, a solution (200 μ L) of **1a''** (3.3 mg, 17 μ mol) was added, the contents were mixed, and the reaction was monitored.

■ ASSOCIATED CONTENT

Data Availability Statement

The data underlying this study are available in the published article and its [Supporting Information](#).

SI Supporting Information

The Supporting Information is available free of charge at <https://pubs.acs.org/doi/10.1021/acsorginorgau.3c00013>.

Reaction kinetic data and NMR spectral characterization data ([PDF](#))

■ AUTHOR INFORMATION

Corresponding Author

Nicole S. Sampson – Department of Chemistry, Stony Brook University, Stony Brook, New York 11794-3400, United States; orcid.org/0000-0002-2835-7760; Email: Nicole.sampson@stonybrook.edu

Author

Francis O. Boadi – Department of Chemistry, Stony Brook University, Stony Brook, New York 11794-3400, United States; orcid.org/0000-0002-2064-5151

Complete contact information is available at: <https://pubs.acs.org/doi/10.1021/acsorginorgau.3c00013>

Author Contributions

Credit: **Francis O Boadi** conceptualization (equal), formal analysis (lead), investigation (lead), validation (lead), writing-original draft (lead), writing-review & editing (equal); **Nicole S Sampson** conceptualization (equal), funding acquisition (lead), methodology (lead), project administration (lead), resources (lead), supervision (lead), writing-review & editing (equal).

Notes

The authors declare no competing financial interest.

■ ACKNOWLEDGMENTS

This research is funded by NSF CHE1609494 (N.S.S.), NIH R01GM097971 (N.S.S.), NIHR35GM145247 (N.S.S.), and NIH T32GM092714 (F.O.B.).

■ REFERENCES

- (1) Bielawski, C. W.; Grubbs, R. H. Living Ring-Opening Metathesis Polymerization. *Prog. Polym. Sci.* **2007**, *32*, 1–29.
- (2) Sutthasupa, S.; Shiotsuki, M.; Sanda, F. Recent Advances in Ring-Opening Metathesis Polymerization, and Application to Synthesis of Functional Materials. *Polym. J.* **2010**, *42*, 905–915.
- (3) Amass, A. J., Ring-Opening Metathesis Polymerization of Cyclic Alkenes. In *New Methods of Polymer Synthesis*; Ebdon, J. R., Ed. Springer US: Boston, MA, 1991; pp. 76–106, DOI: 10.1007/978-1-4684-1530-8_3.
- (4) Gutierrez, S.; Fulgencio, A.; Tlenkopatchev, M. A. Density Functional Theory Study of Ring-Chain Equilibria for the Cross-Metathesis of Cyclohexene and cis,cis-Cycloocta-1,5-diene with Functionalized Olefins. *J. Chem. Thermodyn.* **2006**, *38*, 383–387.
- (5) Song, A.; Parker, K. A.; Sampson, N. S. Synthesis of Copolymers by Alternating ROMP (AROMP). *J. Am. Chem. Soc.* **2009**, *131*, 3444–3445.
- (6) Tan, L.; Parker, K. A.; Sampson, N. S. A Bicyclo[4.2.0]octene-Derived Monomer Provides Completely Linear Alternating Copolymers via Alternating Ring-Opening Metathesis Polymerization (AROMP). *Macromolecules* **2014**, *47*, 6572–6579.
- (7) Elling, B. R.; Xia, Y. Living Alternating Ring-Opening Metathesis Polymerization Based on Single Monomer Additions. *J. Am. Chem. Soc.* **2015**, *137*, 9922–9926.
- (8) Sun, H.; Liang, Y.; Thompson, M. P.; Gianneschi, N. C. Degradable Polymers via Olefin Metathesis Polymerization. *Prog. Polym. Sci.* **2021**, *120*, No. 101427.
- (9) Sui, X.; Zhang, T.; Pabara, A. B.; Fu, L.; Gutekunst, W. R. Alternating Cascade Metathesis Polymerization of Enynes and Cyclic Enol Ethers with Active Ruthenium Fischer Carbenes. *J. Am. Chem. Soc.* **2020**, *142*, 12942–12947.
- (10) Park, H.; Choi, T.-L. Fast Tandem Ring-Opening/Ring-Closing Metathesis Polymerization from a Monomer Containing Cyclohexene and Terminal Alkyne. *J. Am. Chem. Soc.* **2012**, *134*, 7270–7273.
- (11) Tan, L.; Li, G.; Parker, K. A.; Sampson, N. S. Ru-Catalyzed Isomerization Provides Access to Alternating Copolymers via Ring-Opening Metathesis Polymerization. *Macromolecules* **2015**, *48*, 4793–4800.
- (12) Li, G.; Sampson, N. S. Alternating Ring-Opening Metathesis Polymerization (AROMP) of Hydrophobic and Hydrophilic Monomers Provides Oligomers with Side-Chain Sequence Control. *Macromolecules* **2018**, *51*, 3932–3940.
- (13) Boadi, F. O.; Sampson, N. S. Gradient Copolymer Prepared from Alternating Ring-Opening Metathesis of Three Monomers. *Polym. Chem.* **2021**, *12*, 5613–5622.
- (14) Boadi, F. O.; Zhang, J.; Yu, X.; Bhatia, S. R.; Sampson, N. S. Alternating Ring-Opening Metathesis Polymerization Provides Easy Access to Functional and Fully Degradable Polymers. *Macromolecules* **2020**, *53*, 5857–5868.
- (15) Tashiro, K.; Akiyama, M.; Kashiwagi, K.; Okazoe, T. The Fluorocarbene Exploit: Enforcing Alternation in Ring-Opening Metathesis Polymerization. *J. Am. Chem. Soc.* **2023**, *145*, 2941–2950.
- (16) Zhang, J.; Yu, X.; Zheng, B.; Shen, J.; Bhatia, S. R.; Sampson, N. S. Cationic Amphiphilic Alternating Copolymers with Tunable Morphology. *Polym. Chem.* **2020**, *11*, 5424–5430.
- (17) Choi, T.-L.; Lee, C. W.; Chatterjee, A. K.; Grubbs, R. H. Olefin Metathesis Involving Ruthenium Enic Carbene Complexes. *J. Am. Chem. Soc.* **2001**, *123*, 10417–10418.
- (18) Fomine, S.; Tlenkopatchev, M. A. Ring-Opening of Cyclohexene via Metathesis by Ruthenium Carbene Complexes. A Computational Study. *Organometallics* **2007**, *26*, 4491–4497.
- (19) Ulman, M.; Belderrain, T. R.; Grubbs, R. H. A series of Ruthenium (II) Ester-Carbene Complexes as Olefin Metathesis Initiators: Metathesis of Acrylates. *Tetrahedron Lett.* **2000**, *41*, 4689–4693.
- (20) Youn, G.; Sampson, N. S. Substituent Effects Provide Access to Tetrasubstituted Ring-Opening Olefin Metathesis of Bicyclo[4.2.0]oct-6-enes. *ACS Org. Inorg. Au* **2021**, *1*, 29–36.
- (21) Corbett, J. F. Pseudo First-Order Kinetics. *J. Chem. Educ.* **1972**, *49*, 663.
- (22) Nelson, D. J.; Manzini, S.; Urbina-Blanco, C. A.; Nolan, S. P. Key Processes in Ruthenium-Catalysed Olefin Metathesis. *Chem. Commun.* **2014**, *50*, 10355–10375.
- (23) Bielawski, C. W.; Grubbs, R. H. Increasing the Initiation Efficiency of Ruthenium-Based Ring-Opening Metathesis Initiators: Effect of Excess Phosphine. *Macromolecules* **2001**, *34*, 8838–8840.
- (24) Cater, H. L.; Balynska, I.; Allen, M. J.; Freeman, B. D.; Page, Z. A. User Guide to Ring-Opening Metathesis Polymerization of endo-Norbornene Monomers with Chelated Initiators. *Macromolecules* **2022**, *55*, 6671–6679.
- (25) Martinez, H.; Miró, P.; Charbonneau, P.; Hillmyer, M. A.; Cramer, C. J. Selectivity in Ring-Opening Metathesis Polymerization of Z-Cyclooctenes Catalyzed by a Second-generation Grubbs Catalyst. *ACS Catal.* **2012**, *2*, 2547–2556.
- (26) Su, J. K.; Jin, Z.; Zhang, R.; Lu, G.; Liu, P.; Xia, Y. Tuning the Reactivity of Cyclopropenes from Living Ring-Opening Metathesis Polymerization (ROMP) to Single-Addition and Alternating ROMP. *Angew. Chem., Int. Ed.* **2019**, *58*, 17771–17776.
- (27) Hoff, E. A.; De Hoe, G. X.; Mulvaney, C. M.; Hillmyer, M. A.; Alabi, C. A. Thiol–Ene Networks from Sequence-Defined Polyurethane Macromers. *J. Am. Chem. Soc.* **2020**, *142*, 6729–6736.
- (28) Jakubowski, W.; Juhari, A.; Best, A.; Koynov, K.; Pakula, T.; Matyjaszewski, K. Comparison of Thermomechanical Properties of Statistical, Gradient and Block Copolymers of Isobornyl Acrylate and N-Butyl Acrylate with Various Acrylate Homopolymers. *Polymer* **2008**, *49*, 1567–1578.
- (29) Yuan, W.; Mok, M. M.; Kim, J.; Wong, C. L. H.; Dettmer, C. M.; Nguyen, S. T.; Torkelson, J. M.; Shull, K. R. Behavior of Gradient Copolymers at Liquid/Liquid Interfaces. *Langmuir* **2010**, *26*, 3261–3267.
- (30) Mayo, F. R.; Walling, C. Copolymerization. *Chem. Rev.* **1950**, *46*, 191–287.
- (31) Beckingham, B. S.; Sanoja, G. E.; Lynd, N. A. Simple and Accurate Determination of Reactivity Ratios Using a Nonterminal Model of Chain Copolymerization. *Macromolecules* **2015**, *48*, 6922–6930.
- (32) Gleede, T.; Markwart, J. C.; Huber, N.; Rieger, E.; Wurm, F. R. Competitive Copolymerization: Access to Aziridine Copolymers with Adjustable Gradient Strengths. *Macromolecules* **2019**, *52*, 9703–9714.
- (33) Love, J. A.; Morgan, J. P.; Trnka, T. M.; Grubbs, R. H. A Practical and Highly Active Ruthenium-Based Catalyst that Effects the Cross Metathesis of Acrylonitrile. *Angew. Chem., Int. Ed.* **2002**, *41*, 4035–4037.